RSC Advances

PAPER

View Article Online
View Journal | View Issue

Cite this: *RSC Adv.*, 2024, **14**, 6642

Protection against myocardial ischemia/reperfusion injury in mice by 3-caffeoylquinic acid isomers isolated from *Saxifraga tangutica*†

Yingying Tong,[ab] Gang Li,[b] Xiaobing Shi,[b] Lin Wang,[b] Jia Zhou,[ab] Ming Chu,[b] Zhenhua Wang,[b] A. M. Abd El-Aty[cd] and Jun Dang*[a]

The development of ischemic heart disease (IHD) involves a variety of pathophysiological responses, such as mitochondrial dysfunction. Many compounds with antioxidant activity isolated from natural products have been shown to have significant effects on the prevention and treatment of cardiovascular diseases. However, little is known about the palliative effects of 3-caffeoylquinic acid isomers isolated from *Saxifraga tangutica* (*S. tangutica*) on myocardial ischemia/reperfusion injury (MIRI). Three isomers of 3-caffeoylquinic acid were isolated from *S. tangutica* and identified as neochlorogenic acid (Fr2-4-1-1, 18.5 mg), chlorogenic acid (Fr2-5-1-1, 81.7 mg) and cryptochlorogenic acid (Fr2-5-2-1, 15.0 mg) using medium-pressure liquid chromatography-high-pressure two-dimensional liquid chromatography. An *in vitro* DPPH assay showed that cryptochlorogenic acid (CCGA), neochlorogenic acid (NCGA) and chlorogenic acid (CGA) (in order of activity from strongest to weakest) possessed superior antioxidant activity. Langendorff's *in vitro* model was utilized to explore the protective effects of 3 caffeoylquinic acid isomers against MIRI. The *ex vivo* MIRI assay demonstrated that CCGA significantly improved hemodynamic function ($P < 0.05$), hemodynamic function-related indices (LVDP, RPP, +dP/dt and −dP/dt), and cell morphology in I/R myocardium tissues. In addition, the results of western blot analysis showed that mitochondrial biogenesis was significantly increased in I/R myocardial tissues after treatment with CCGA. In contrast, the activities of CGA and NCGA were lower. This is the first demonstration of efficient preparative isolation of 3-caffeoylquinic acid isomers (CGA, NCGA and CCGA) from *S. tangutica*. CCGA may be a promising approach for the treatment of cardiac I/R injury, especially for the regulation of mitochondrial biogenesis after MIRI.

Received 3rd January 2024
Accepted 11th February 2024

DOI: 10.1039/d4ra00046c

rsc.li/rsc-advances

1 Introduction

Cardiovascular disease is now a global public health problem, and ischemic heart disease (IHD) is one of the leading causes of cardiovascular death.[1] Ischaemia/reperfusion (I/R) therapy is an effective means of relieving sudden ischemic events, restoring blood supply to the ischemic myocardium and reducing the risk of death when treated early.[2] However, when blood provided to the myocardium is interrupted and restored within a certain period of time, it can lead to abnormal left ventricular function, which in turn can cause severe damage to the original ischemic myocardium, *i.e.*, myocardial ischemia/reperfusion injury (MIRI).[3] Furthermore, the duration of ischaemia is positively correlated with the degree of myocardial damage.[4] Mitigating the damage caused to organisms during IR therapy is a key component of treating cardiovascular disease (CVD).

MIRI results in complex pathophysiologic symptoms while improving the myocardial blood supply. These pathophysiologic responses involve a variety of molecular processes, such as oxidative stress,[5] inflammation,[6] iron death,[7] and mitochondrial dysfunction.[8] Mitochondria are important organs for energy production in cardiomyocytes. Mitochondrial function is closely related to cardiac development and disease processes, and proper mitochondrial functioning depends on the dynamic balance of mitochondrial regulation (processes such as mitochondrial biogenesis, division and fusion, and autophagy).[9] Mitochondrial biogenesis, fission and fusion not only increase the quality and quantity of mitochondria in cells to meet their energy demand but also promote the recovery of cardiomyocytes from MIRI to improve cardiac function.[10] The

[a]*Qinghai Provincial Key Laboratory of Tibetan Medicine Research, Key Laboratory of Tibetan Medicine Research, Northwest Institute of Plateau Biology, Chinese Academy of Sciences, Xining 810001, Qinghai, China. E-mail: dangjun@nwipb.cas.cn; Fax: +86-971-6143282; Tel: +86-971-6143282*

[b]*Center for Mitochondria and Healthy Aging, College of Life Sciences, Yantai University, Yantai 264005, China*

[c]*Department of Pharmacology, Faculty of Veterinary Medicine, Cairo University, Giza 12211, Egypt*

[d]*Department of Medical Pharmacology, Faculty of Medicine, Atatürk University, Erzurum 25240, Turkey*

† Electronic supplementary information (ESI) available. See DOI: https://doi.org/10.1039/d4ra00046c

sirtuin family is located in the mitochondria, and sirt1 is a member of the sirtuin family. Many studies have shown that MIRI can be attenuated by activating the sirt1/PGC-1α signalling pathway.[11–13] Therefore, identifying molecules that can attenuate mitochondrial dysfunction is a possible strategy for treating of myocardial injury caused by I/R.

Saxifraga tangutica (*S. tangutica*) is a renascent herb remaining with the *Saxifraga* genus in the family Saxifragaceae and is one of the commonly used traditional Tibetan medicines (TTMs).[14] *S. tangutica* is bitter and cold in taste and is used to clear the heat of liver and gallbladder fever and to treat acute otitis media.[15] *S. tangutica* extract can effectively inhibit the growth of human gastric cancer cells, promote the apoptosis of gastric cancer cells, and inhibit the growth of thyroid tumors.[16] Flavonoids and phenylpropanoids are the main bioactive components of *S. tangutica*, and have anti-inflammatory, antioxidant, anticancer and other biological activities.[17] Moreover, the simultaneous isolation and identification of chlorogenic acid (CGA), neochlorogenic acid (NCGA), and cryptochlorogenic acid (CCGA) from *S. tangutica* have not been performed. The bioactivities of these three isomers differ depending on their structures. In terms of its ability to ameliorate cardiac hypertrophy, CCGA was found to be the most effective treatment, followed by NCGA and CGA.[18] CCGA which has a 4-ester group structure has the strongest ability to form hydrogen bonds and a more stable complex with human serum albumin.[19] Both NCGA and CCGA inhibited pancreatic lipase, while NCGA had a better effect on the structure of pancreatic lipase.[20] CCGA reduces blood glucose in rats by activating the cystine/glutamate transporter system/glutathione peroxidase 4/Nrf2 to inhibit ferroptosis *in vivo*.[21] CCGA inhibited the downregulation of the H_2O_2-related antiapoptotic proteins Bcl-2 and Bcl-X_L while blocking the H_2O_2-induced proapoptotic cleavage of caspase-3 and poly(ADP-ribose) polymerase, inducing the expression of NQO1 and thereby protecting neuronal cells.[22]

3-Caffeoylquinic acid isomers are widely known for their good antioxidant activity and are popular molecules for the treatment of diseases.[23,24] How to obtain these products rapidly from complex natural products is a problem worth exploring and solving. The traditional method of activity-directed separation by open-column chromatographic elution combined with *in vitro* activity detection is labor intensive, time consuming, and costly.[25] The complexity of the components of TTMs increases the difficulty of separation compounds. With the continuous development of chromatography, the separation of chemical components has been realized due to the different retention mechanisms between of different systems.[26] The difference in the selectivity of chemical components between reversed-phase liquid chromatography (RPLC) and hydrophilic liquid chromatography (HILIC) provides additional possibilities for separation.[27]

In this study, active chromatographic peaks (1,1-diphenyl-2-picrylhydrazyl (DPPH) radical inhibitors) were identified, and 3-caffeoylquinic acid isomer radical inhibitors were separated in *S. tangutica via* an online HPLC–DPPH system and two-dimensional liquid chromatography (RPLC and HILIC). DPPH *in vitro* bioactivity tests were performed to further verify the antioxidant activity of the isolated compounds and to analyse the conformational relationship between the structure and activity of the 3-caffeoylquinic acid isomers. The Langendorff device was used to establish an isolated MIRI model to detect the hemodynamic indices of the relevant myocardium, to observe the results of H&E-stained sections and to analyse the expression of proteins related to mitochondrial biogenesis (sirt1, PGC-1α, Nrf1, Mfn2, and Drp1) and to comparatively discuss the differences between the protective effects of the 3-caffeoylquinic acid isomers on MIRI. In this paper, we report for the first time the recognition and isolation of 3-caffeoylquinic acid isomer free radical inhibitors from *S. tangutica* in the family Saxifragaceae. This on-line activity recognition and targeted recognition and isolation method provides new ideas for the isolation of free radical inhibitors from other plants or even for the isolation of enzyme inhibitors. The aim of this study was to clarify the mitigating effect of 3-caffeoylquinic acid isomers on MIRI, to analyse the underlying mechanisms from the perspective of mitochondrial function, and to provide valuable information for the clinical treatment of MIRI.

2 Experimental

2.1 Chemicals and reagents

Preparation-grade ethanol (EtOH), preparation-grade methanol (MeOH) and preparation-grade acetonitrile (ACN) were obtained from Zhengzhou Paini Chemical Reagent Factory (Henan, China). HPLC-grade EtOH, HPLC-grade MeOH, and HPLC-grade ACN were obtained from the Shanxi Xian SHUNDA Chemical Reagent Instrument. Formic acid (FA) was obtained from Shanghai McLean Biochemical Technology Co. (China). HPLC-grade water was prepared using a Moore water purification system (Chongqing, China). DPPH chemicals were purchased from Sigma–Aldrich (Steinheim, Germany). Oleic acid (OA) was obtained from Aladdin Industrial Co. (Shanghai, China). The following items were subsequently procured from the specified commercial sources: anti-Drp1 (Abcam, ab184247), anti-Mfn2 (Abcam, ab56889), anti-GAPDH (Abcam, ab8245), anti-sirt1 (Cell Signalling, 8469S), anti-PGC-1α (Cell Signalling, 2178S), anti-Nrf1 (Cell Signalling, 46743S), anti-TFAM (Thermo Fisher Scientific, MA5-16148), goat anti-rabbit IgG-HRP (ZSGB-Bio, ZB-5301) and goat anti-mouse IgG-HRP (ZSGB-Bi, ZB-2305).

2.2 Plant material and animals

Saxifraga tangutica: for example, from *S. tangutica*, the whole herb was collected from Guoluo (geographic coordinate: 34° 33′37.08″N, 99°47′35.16″E, Qinghai, China) and confirmed to be the Sect. *Micranthae* of the *Saxifraga* genus within the Saxifragaceae family by Professor Lijuan Mei (Northwest Institute of Plateau Biology, Chinese Academy of Sciences). The certificate specimen (herbarium code: 0325734) was stored in the Tibetan Plateau Museum of Biology.

Healthy adult male specific pathogen-free (SPF)-grade ICR mice weighing 25–30 g were obtained from Jinan Pengyue Experimental Animal Breeding Co., Ltd (Jinan, China). Mice

were cared for according to the 2011 8th edition of the Guidelines for the Care and Use of Laboratory Animals (US National Institutes of Health). The experimental procedures were approved by the Laboratory Animal Welfare Ethics Review Committee of Yantai University (No. YDLL2023M126). SPF-grade ICR mice were fed in a rearing room under the following conditions: ambient temperature of 22 ± 3 °C and relative humidity of 40–70%.

2.3 Preparation of the MeOH extract of the *S. tangutica* sample and preparation of the *S. tangutica* Fr2 sample

MeOH extraction of the *S. tangutica* sample: the shade-dried *S. tangutica* herb was soaked in MeOH (4.0 L once) for 24 h (24 h once, three times in total). Subsequently, the samples were filtered. The filtrate was mixed (12.0 L) and concentrated (100 rpm) in a negative pressure and 40 °C water bath to approximately 300.0 mL.

Preparation of the *S. tangutica* Fr2 sample: 300.0 mL of the concentrate was mixed with 200.0 g of dried polyamide, and the mixture was dried in an oven. The sample-polyamide mixture weighted 265.0 g. The mixture was loaded into a medium-pressure column (49 × 100 mm), which was subsequently connected to a medium-pressure column (49 × 460 mm) packed with MCI GEL® CHP20P packing material and later prepared by a medium-pressure liquid chromatography (MPLC) system (Hanbon Sci. & Tech.). The mobile phase comprised H_2O (A) and EtOH (B). Gradient elution was used to set up the chromatographic conditions: 0–120 minutes, 0–100% B, 120–150 minutes, 100% B. A total of 22.0 g of each injection (repeated 12 times) was eluted with a flow velocity of 30.0 mL min^{-1} at 254 nm. Six fractions were obtained and labelled Fr1–Fr6. The target Fr2 was obtained (2.84 g) through concentration and freeze-drying.

2.4 Identification of chromatographic peaks indicating DPPH radical inhibitor activity in the Fr2 sample

A sample of *S. tangutica* Fr2 was assayed using an online HPLC–DPPH system, with some modifications based on previous descriptions.[28] Dissolution of 2.84 g of the Fr2 sample with a 50.0 mL 50% MeOH–H_2O mixture (*v*/*v*) yielded a 56.8 mg mL^{-1} solution of Fr2 (after filtration through a 0.22 μm filter film). The target fraction Fr2 sample was analysed using ReproSil-Pur C18 AQ (4.6 × 250 mm, 5 μm) on an HPLC (LC-16A, Shimadzu) instrument at an elution rate of 1.0 mL min^{-1}. The mobile phase consisted of 0.2% FA aqueous solution (A) and HPLC-grade ACN (B). The linear gradient analysis conditions were as follows: 0–60 min, 0–22% B. With the column temperature maintained at 25 °C, 5 μL of the Fr2 sample was transferred into the HPLC–DPPH system, and the absorbance of the HPLC section was measured at 254 nm. After the Fr2 sample was partially separated by HPLC, the eluent (containing both antioxidant and nonantioxidant components) was removed in an orderly manner. The HPLC-analysed sample was reacted with DPPH EtOH solution (25 μg mL^{-1}) through an 18 m long reaction coil. The DPPH EtOH solution was mixed at a flow rate of 0.8 mL min^{-1}. The antioxidant components bind to the DPPH solution, decreasing the amount of DPPH. A decrease in the amount of DPPH results in a decreased absorption, with an inverted peak detected at 517 nm *via* HPLC.

2.5 Preparative isolation of DPPH inhibitors from the *S. tangutica* Fr2 sample

The Fr2 sample was prepared and separated on a laboratory-made Spherical C18 column (50 × 500 mm, 50 μm) with mobile phase A (H_2O) and mobile phase B (MeOH). The final elution procedure for the Fr2 sample was 5% B to 55% B for 80 min. The flow velocity was 70.0 mL min^{-1}. The target sample Fr2 was injected with 10.0 mL at a time into the column by an injection needle for separation, and the absorbance was recorded at 254 nm. Five repetitions of the sample were performed to obtain two active fractions (Fr2-4 358.6 mg and Fr2-5 452.2 mg).

Fr2-4 and Fr2-5 samples separated by the Sphercial C18 stationary phase were further separated on Reprosil-Pur C18 AQ (20 × 250 mm, 5 μm). The mobile phases for both the Fr2-4 and Fr2-5 separations were 0.2% FA aqueous solution (A) and ACN (B). The mobile phases for Fr2-4 (dissolved in 20% MeOH aqueous solution [20 : 80 ν_{MeOH}/ν_{H_2O}], total solution volume 10.0 mL) and Fr2-5 (dissolved in 50% MeOH aqueous solution [50 : 50 ν_{MeOH}/ν_{H_2O}], total solution volume 15.0 mL) were eluted using an isocratic elution procedure with the following elution conditions: (1) 0–30 min, 8% B; (2) 0–30 min, 9% B. The volume of each sample and the amount of each sample of Fr2-4 and Fr2-5 were 0.2% FA aqueous solution (A) and ACN (B), respectively. Fr2-5 had the same volume of each sample and elution flow rates of 1.0 mL and 19.0 mL min^{-1}, respectively. Chromatograms were recorded at 254 nm. Fr2-4-1 (52.2 mg), Fr2-5-1 (132.1 mg) and Fr2-5-2 (39.0 mg) were ultimately obtained.

Further separation of the DPPH inhibitors was achieved by using Click XIon (20 × 250 mm, 5 μm) against Fr2-4-1 (dissolved in MeOH solution, total solution volume 3.0 mL), Fr2-5-1 (dissolved in MeOH solution, total solution volume 8.0 mL), and Fr2-5-2 (dissolved in MeOH solution, total solution volume 5.0 mL) under RP C18 column preparation. The mobile phases were 0.2% FA aqueous solution (A) and ACN (B), the elution process of Fr2-4-1 was from 0 min to 30 min at 92% B with an injection volume of 0.5 mL, and that of Fr2-5-1 was from 0 min to 20 min at 92% B with an infusion volume of 1.0 mL, while the elution process of Fr2-5-2 was from 0 min to 25 min at 92% B with an infusion volume of 1.0 mL. The flow rate of preparation and elution was 19.0 mL min^{-1}, and the chromatograms were collected at 254 nm.

2.6 Purity analysis using online HPLC–DPPH and bioassays against *in vitro* DPPH inhibitors

2.6.1 Purity analysis using online HPLC–DPPH for DPPH inhibitors. The purity of the isolated DPPH inhibitors was evaluated on a ReproSil-Pur C18 AQ (4.6 × 250 mm, 5 μm) stationary phase using an online HPLC–DPPH system. The antioxidant activity of the compounds was also verified. (1) Analytical conditions for the HPLC were as follows: 0–60 min, 0–22% B; flow rate, 1.0 mL min^{-1}; and detection wavelength, 254 nm. A is a 0.2% FA aqueous solution, B is ACN, and A and B

are the mobile phases for chromatographic analysis. The injection volume was 5 μL. (2) Analytical conditions for the DPPH fraction: 0–60 min 100% DPPH solution (dissolved in EtOH at a concentration of 25 μg mL^{-1}) at a flow velocity of 0.8 mL min^{-1} and a detection wavelength of 517 nm.

2.6.2 ***In vitro*** **DPPH assay.** DPPH radical scavenging ability was determined with a light absorption full-wavelength enzyme labelling apparatus (Shanghai Flash Spectrum Biotechnology, China) based on the procedure described in Dehghan *et al.* with appropriate modifications.[29] The isolated compounds were prepared at different concentrations (0–100 μM) in 50% EtOH/H_2O solution. The DPPH solution was prepared with the same solution at a concentration of 63 μM. A fixed volume of 60.0 μL of the sample solution and a fixed volume of 140.0 μL of the DPPH solution were mixed in a 96-well plate (Wuxi NEST Biotechnology Co., Ltd) and reacted for 20 min at 37 °C in the dark, after which the absorbance was measured at 517 nm. The experiment was performed three times with the same operation tautologically. The expression of DPPH radical scavenging activity was $(1 - (A_t - A_1)/A_0) \times 100\%$. A_t is the absorbance in the experimental group (with sample plus DPPH), A_1 is the absorbance in the control group (sample without DPPH) and A_0 is the absorbance in the blank group (DPPH without sample).

2.7 Ischemia/reperfusion (I/R) injury model in Langendorff-perfused mouse hearts

Mouse hearts were prepared for Langendorff perfusion and I/R as previously described.[30] Briefly, hearts from male ICR mice were rapidly excised and retrogradely perfused with Krebs–Henseleit buffer (K–H buffer: 119 mmol L^{-1} NaCl, 4.7 mmol L^{-1} KCl, 1.2 mmol L^{-1} KH_2PO_4, 1.2 mmol L^{-1} $MgSO_4$, 22 mmol L^{-1} $NaHCO_3$, 11 mmol L^{-1} glucose, 0.5 mmol L^{-1} EDTA, 2.5 mmol L^{-1} $CaCl_2$, 1% BSA, 0.8 mmol L^{-1} oleic acid, 50 μU mL^{-1} insulin, pH 7.4 and gassed with 5% CO_2 in O_2) at 37 °C using the Langendorff technique at a constant pressure of 80 mm_{Hg}. Left ventricular (LV) pressure was monitored using a water-filled balloon linked to a pressure transducer (Chengdu Taimeng Instrument, Sichuan, China) which was inserted into the LV cavity to achieve a left ventricular end-diastolic pressure (LVEDP) between 5 and 10 mm_{Hg}. Left ventricular developed pressure (LVDP), maximal rates of pressure development over time ($+dP/dt_{max}$) maximal pressure decay over time ($-dP/dt_{max}$), and maximal heart rate were monitored with a bioinformation acquisition system (Chengdu Taimeng Instrument). CGA, NCGA, or CCGA were added to the perfusate at a final concentration of 5.0 μM 15 min before ischaemia, after which the hearts were placed under ischaemia conditions by stopping perfusion for 25 min and subjected to reperfusion for 45 min. At the end of reperfusion, the hearts were rapidly removed and frozen in liquid nitrogen for western blot analysis.

2.8 Histological evaluation

After 25 minutes of cardiac ischemia and 45 minutes of reperfusion, the hearts were carefully extracted and immersed in 4% paraformaldehyde (PFA) for preservation. After adequate fixation, the hearts were dehydrated and embedded in paraffin. Paraffin sections (5 μm) of the myocardial tissue were then subjected to hematoxylin and eosin staining. This staining method allowed for a detailed evaluation of the cardiac tissue using light microscopy.

2.9 Western blotting

After recovery from −80 °C storage, the heart tissues were ground, incubated in ice-cold RIPA buffer containing phenylmethanesulfonyl fluoride (PMSF) for 30 min and subsequently cleared by centrifugation at 12 000×*g* for 20 min at 4 °C. The protein concentration was measured with a BCA protein assay kit (No. P0012, Beyotime Biotechnology). Equivalent amounts of total protein were mixed with 5× sodium dodecyl sulfate–polyacrylamide gel electrophoresis (SDS–PAGE) sample buffer and boiled. The same amounts of protein were subjected to SDS–PAGE, transferred to a polyvinylidene fluoride membrane and blocked at room temperature for 1 h. For immunoblotting, the primary antibodies were applied at 4 °C overnight, followed by incubation with the secondary antibody at room temperature for 1 h. Western blot analysis was performed using anti-Drp1, anti-Mfn2, anti-sirt1, anti-PGC-1α, anti-Nrf1, anti-TFAM, and anti-GAPDH antibodies. The band intensities were detected by enhanced chemiluminescence and quantified with Image-Pro Plus 6.0 software (Media Cybernetics, USA).

2.10 Statistical analyses

Each experimental replication was performed independently three times. The data are expressed as the mean ± standard error of the mean (SEM) and were normally distributed. DPPH clearance capacity was statistically analysed using IBM SPSS Statistics version 23 software, and Student's *t*-test was performed for statistical analysis using GraphPad Prism 8.0 (GraphPad Software, Inc., San Diego, CA, USA). Analysis of variance (ANOVA) was used to analyse significant differences between groups. Differences were considered to be statistically significant when the *P* value was <0.05 ($^*P < 0.05$).

3 Results and discussion

3.1 Sample pretreatment and screening of free radical inhibitors in the *S. tangutica* Fr2 sample

In this study, one of the conventional extraction methods, maceration, was chosen for the extraction of *S. tangutica*. Compared with other extraction methods, maceration is easy to perform, has simple equipment, and widely meets the extraction needs of different herbs without destroying the internal structure of secondary metabolites in the plant.[31] Chuah *et al.* extracted *Clinacanthus nutans* leaves by maceration, Soxhlet extraction and magnetic stirring methods, in which the extracts obtained by the maceration method retained the antioxidant activity of *Clinacanthus nutans* leaves to a greater extent.[32] Based on the high solubility, low boiling point and low cost of MeOH, MeOH was chosen as the solvent for the present extraction. A total of 500.0 g of shade-dried *S. tangutica* whole herb was extracted with MeOH to obtain 65.0 g of crude sample for an extraction rate of 13%. MCI GEL® CHP20P was used as the

stationary phase and MeOH/H_2O system for fractionation and pretreatment of the *S. tangutica* crude extract. MCI GEL® CHP20P packing is based on polystyrene and divinyl copolymer and is suitable for salient separations. It is chemically stable and adaptable to eluents with different pH values. A dry mixture of polyamide and extract was loaded into a medium-pressure column and processed by an MCI GEL® CHP20P stationary phase and preparative liquid chromatography system to obtain six fractions after 12 replicate preparations (as shown in Fig. 1A2). The solid injection method replaces the liquid injection method, which greatly improves the loading capacity of the preparative chromatography system and shortens the working time (the actual schematic diagram of the system connection is shown in Fig. 1A1). In addition, visualization of the separation enables the reliability and traceability of each step of the separation. Fr2 (2.84 g, 4.3% recovery) was chosen as the target fraction for separating the 3-caffeoylquinic acid isomer from the DPPH inhibitors in the subsequent process.

The online HPLC–DPPH technique was used to screen for DPPH inhibitors in the pretreated Fr2 sample. During preparation, selecting the most appropriate chromatographic separation conditions for performing online HPLC–DPPH is a crucial step. Following this, using preestablished chromatographic conditions, the Fr2 sample was isolated through HPLC (using a ReproSil-Pur C18 AQ column) and reacted with DPPH radicals postcolumn reactions, taking place at a length of 18 m. The reaction of Fr2 with DPPH radicals was identified at 517 nm, and some of the chromatographic peaks showed a decrease in absorbance and inverted peaks. The identification chromatograms are shown in Fig. 1B2 and B3 (Fig. 1B1 is a schematic and actual diagram of the online RPLC-DPPH system). As demonstrated in Fig. 1B2 and B3, the retention time of the Fr2 sample showed three main DPPH inhibitor peaks between 30 min and 45 min (negative peaks a–c in Fig. 1B3 correspond to hearts 1–3 in Fig. 1B2).

Based on the analytical obtained for Fr2 on the RP C18 column (Fig. 1B), futher treatment of the Fr2 sample was necessary to alleviate the difficulty of preparative separation and enrichment of the target components. Combined with the previous separation results, the reversed-phase packing material showed good retention performance for the target components, and the Spherical C18 (50 μm) could meet this requirement. Therefore, the preparative liquid chromatography mixture was connected to a column equipped with a Spherical C18. Again, a solid sample was taken, and five fractions (Fr2-1–Fr2-5) were obtained after five medium-pressure preparative separations. The separation chromatograms are shown in Fig. 2A, and indicate that Spherical C18 was effective at separating Fr2. After evaporation of the solvent, 358.6 mg of Fr2-4 and 452.2 mg of Fr2-5 were obtained (recoveries totaled 28.5%). Fractions Fr2-4 and Fr2-5 were redissolved in MeOH/H_2O (20 : 80 *v*/*v*; 10.0 mL and 50 : 50 *v*/*v*; 15.0 mL), respectively, and passed through a 0.22 μm filter prior to the separation step. The redissolved fractions Fr2-4 and Fr2-5 were analysed *via* HPLC (Essentia LC-16A system) using a ReproSil-Pur C18 AQ column, as shown in Fig. 2B. Fig. 2B1–B3 shows the analytical chromatograms associated with sample Fr2 and fractions Fr2-4 and Fr2-5. Compared with those in Fig. 2B1 to B3, the three

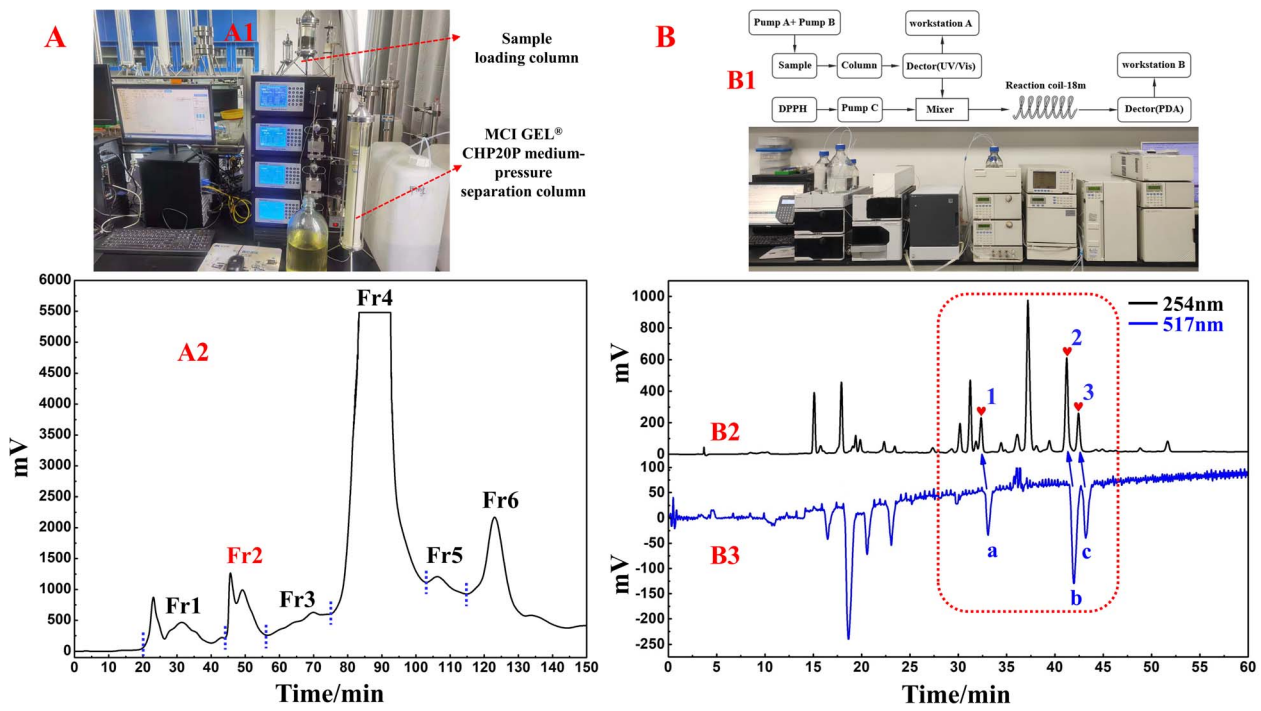

Fig. 1 (A) Schematic diagram (A1) and separation chromatogram (A2) of *S. tangutica* extract with MCI GEL® CHP20P medium-pressure liquid chromatography. (B) Schematic diagram and device diagram of the online HPLC–DPPH activity screening system (B1) and activity screening chromatogram of Fr2 (B2).

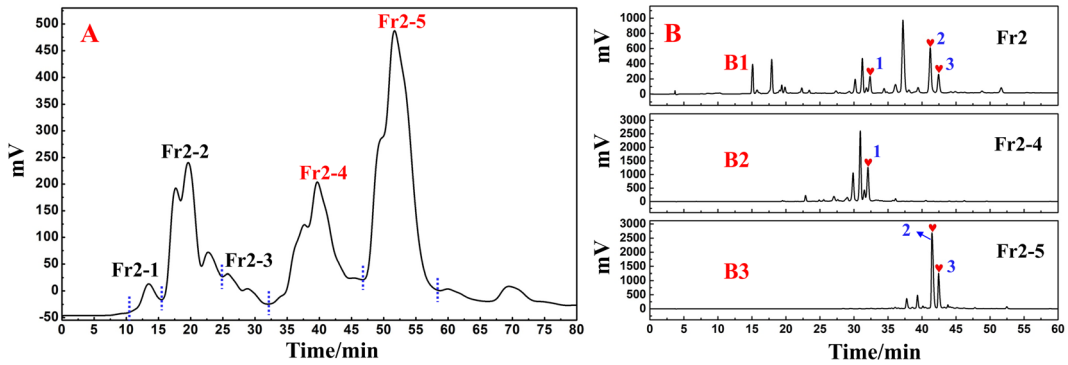

Fig. 2 (A) Pretreatment chromatogram of the *S. tangutica* Fr2 sample with Spherical C18 medium-pressure liquid chromatography. (B) Analytical chromatograms of Fr2, Fr2-4 and Fr2-5.

DPPH inhibitors (peaks 1–3) in the Fr2 crude sample were effectively enriched in the Fr2-4 and Fr2-5 fractions (hearts 1–3 in Fig. 2B2 and B3, respectively). In addition, peaks 1–3 (Fig. 2B2 and B3) were attributed to the three large components of the Fr2 sample (Fig. 2B).

3.2 Target separation of free radical inhibitors from fractions Fr2-4 and Fr2-5 using two-dimensional liquid chromatography

Chromatographic separation conditions were optimized for Fr2-4 and Fr2-5 using the same reversed-phase C18 column (ReproSil-Pur C18 AQ) (Fig. 3A and D). This approach the separation of the chromatographic peaks and the purification efficiency of the target peaks. Based on the optimized separation conditions, the active chromatographic peaks in fraction Fr2-4 and Fr2-5 were identified using an online HPLC–DPPH system. Based on the separation and activity screening of Fr2-4, a high-resolution peak (Fig. 3A) appeared in Fr2-4, corresponding to an inverted peak at 517 nm (Fig. 3B) (peak 1 corresponds to the DPPH negative peak a). In response to the results shown in Fig. 3A and B, a one-dimensional preparation of the DPPH inhibitor in this fraction was performed by linearly scaling up Fr2-4 on a ReproSil-Pur C18 AQ (20 × 250 mm, 5 μm) column at a flow rate of 19.0 mL min^{-1}. The sample volume was 0.7 mL per injection. Fr2-4-1 (52.2 mg, 14.6% recovery) was obtained after 14 replicate preparations. The preparative chromatogram is shown in Fig. 3C. As shown in Fig. 3D, two well-separated peaks were observed for Fr2-5. Peak 2 and peak 3 correspond to negative peak b and negative peak c, respectively, in Fig. 3E. Like for Fr2-4, linear scaling up to a ReproSil-Pur C18 AQ (20 × 250 mm, 5 μm) was performed for one-dimensional preparative separation of the DPPH inhibitors from Fr2-5 with an injection volume of 1.5 mL and a separation rate of 19.0 mL min^{-1}. The target fractions Fr2-5-1 (132.1 mg) and Fr2-5-2 (39.0 mg) were obtained after ten separate preparations with 37.8% recovery. The preparative chromatogram is shown in Fig. 3F.

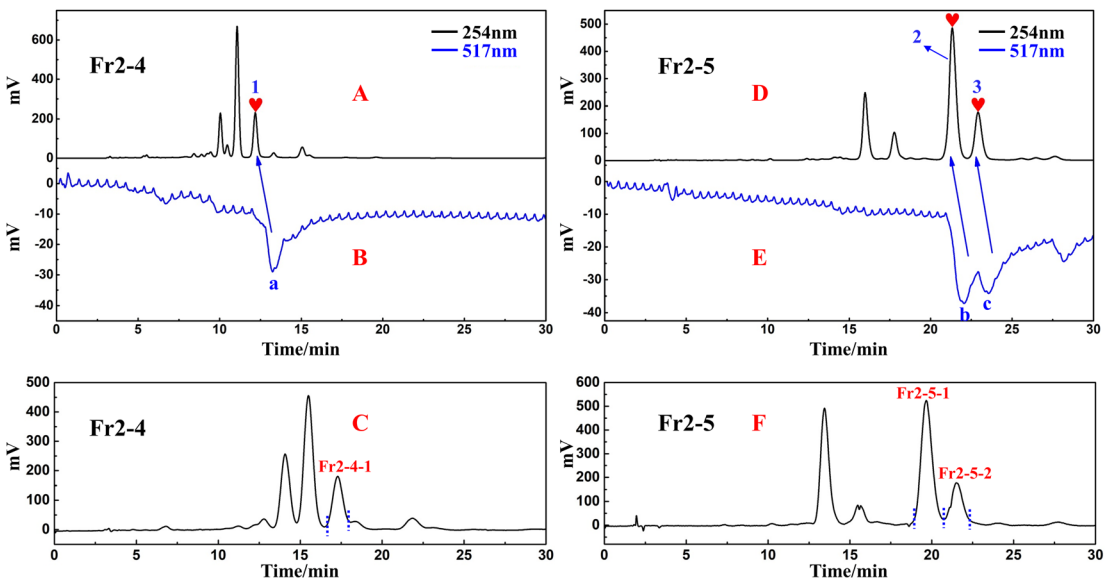

Fig. 3 Optimized analytical chromatogram (A) and (D), DPPH radical scavenging profile (B) and (E) and preparative chromatogram (C) and (F) of fractions Fr2-4 and Fr2-5 on ReproSil-Pur C18 AQ analytical and preparative columns.

Analysed chromatograms of fractions Fr2-4 and Fr2-5 and the three active fractions (Fr2-4-1, Fr2-5-1 and Fr2-5-2) on the ReproSil-Pur C18 AQ analytical column can be found in Fig. 4A–E, respectively. As demonstrated in Fig. 4B, D and E, the fractions Fr2-4-1, Fr2-5-1 and Fr2-5-2 fractions all exhibited one peak with a satisfactory level of purity (>95%) after one-dimensional preparative separation by ReproSil-Pur C18 AQ, which is regarded as a pure compound in traditional separation techniques. However, when fractions Fr2-4-1, Fr2-5-1 and Fr2-5-2 were analysed on a Click XIon (4.6 × 250 mm, 5 μm) column (shown in Fig. 4F, H and J) under optimized conditions, multiple high-resolution peaks (shown by red dashed lines in Fig. 4F, H and J) were identified from these fractions. For fraction Fr2-4-1, the chromatogram included only one main peak (peak 1) from the Click XIon column (Fig. 4F). However, many small peaks were observed at retention times between 15 min and 25 min (red dashed line in Fig. 4F). Similar phenomena occurred in fractions 2-5-1 (Fig. 4H) and 2-5-2 (Fig. 4J). When the above fractions were separated on a ReproSil-Pur C18 AQ column only, some of the overlapping peaks might have precipitated together, preventing easy separation and affecting the purity of the fractions. The well-defined separation of the chromatograms observed was attributed to the distinct differences observed between the two chromatographic columns used, Click XIon and ReproSil-Pur C18 AQ. These data suggest that the Click XIon column can offer complementary selectivity to the ReproSil-Pur C18 AQ column in the purification process of DPPH inhibitors. Therefore, the Click XIon column should be utilized in the second step of the purification process to significantly enhance the isolation and purification of the DPPH inhibitors from the resultant fractions (Fr2-4-1, Fr2-5-1, and Fr2-5-2).

To improve the purity of the three DPPH inhibitors, a second-dimensional purification was conducted on a Click XIon preparative column. Fig. 4G, I and K show the preparative chromatograms of fractions Fr2-4-1, Fr2-5-1 and Fr2-5-2, respectively. After repeating (6, 8 and 5 runs) preparative separations for fractions Fr2-4-1, Fr2-5-1 and Fr2-5-2, the target fractions Fr2-4-1-1, Fr2-5-1-1 and Fr2-5-2-1 (Fig. 4G, I and K) were gathered, and the resulting residues were subsequently dried by evaporating the solvent, resulting in 18.5 mg of Fr2-4-1-1 (recovery 35.4%), 81.7 mg of Fr2-5-1-1 (recovery 61.8%) and 15.0 mg of Fr2-5-2-1 (recovery 38.5%).

The purity and activity of Fr2-4-1-1, Fr2-5-1-1 and Fr2-5-2-1 were reassessed *via* an online RPLC-DPPH system. As shown in Fig. 5A–F, the purities of the DPPH inhibitors were greater than 95%. To elucidate the isolated DPPH inhibitor structures, HR-ESI-MS, ^{1}H NMR, and ^{13}C NMR pattern acquisition were performed, and the results were compared with published data. Upon comparison, it was found that the NMR and MS data of Fr2-4-1-1, Fr2-5-1-1, and Fr2-5-2-1 matched those of NCGA, CGA and CCGA (Fig. 5G–I), and the complete spectra are detailed in the ESI.†

Fraction Fr2-4-1-1 (neochlorogenic acid, ESI-MS *m*/*z* 353.20, $[M-H]^-$, calc. for $C_{16}H_{18}O_9$ *m*/*z* 354.09): ^{1}H NMR (600 M*Hz*, MeOH-d_4) 7.58 (1H, d, $J = 15.9$ *Hz*, H-7′), 7.04 (1H, d, $J = 1.6$ *Hz*, H-2′), 6.93 (1H, dd, $J = 8.2$, 1.6 *Hz*, H-6′), 6.76 (1H, d, $J = 8.2$ *Hz*, H-5′), 6.30 (1H, d, $J = 15.9$ *Hz*, H-8′), 5.35 (1H, q, $J = 3.7$ *Hz*, H-3), 4.14 (1H, td, $J = 9.2$, 4.1 *Hz*, H-5), 3.64 (1H, dd, $J = 8.4$, 3.2 *Hz*, H-4), 2.19 (1H, dd, $J = 14.8$, 3.7 *Hz*, H-2a), 2.13 (2H, m, H-2b, 6a), 1.95 (1H, dd, $J = 13.5$, 9.8 *Hz*, H-6b); ^{13}C NMR (151 M*Hz*, MeOH-d_4) 178.4 (C-7), 169.0 (C-9′), 149.4 (C-4′), 146.8 (C-7′, 3′), 128.0 (C-1′), 122.9 (C-6′), 116.5 (C-5′), 115.8 (C-8′), 115.1 (C-2′), 75.4 (C-1), 74.8 (C-4), 73.0 (C-3), 68.3 (C-5), 41.5 (C-6), 36.7 (C-2). The data correspond to neochlorogenic acid.[33]

Fraction Fr2-5-1-1 (chlorogenic acid, ESI-MS *m*/*z* 353.20, $[M-H]^-$, calc. for $C_{16}H_{18}O_9$ *m*/*z* 354.09): ^{1}H NMR (600 M*Hz*, MeOH-d_4) 7.55 (1H, d, $J = 15.9$ *Hz*, H-7′), 7.04 (1H, d, $J = 2.1$ *Hz*, H-2′), 6.95 (1H, dd, $J = 8.2$, 2.1 *Hz*, H-6′), 6.77 (1H, d, $J = 8.2$ *Hz*, H-5′), 6.25 (1H, d, $J = 15.9$ *Hz*, H-8′), 5.32 (1H, td, $J = 9.2$, 4.4 *Hz*, H-5), 4.16 (1H, m, H-3), 3.71 (1H, m, H-4), 2.01–2.24 (4H, m, H-2, 6); ^{13}C NMR (151 M*Hz*, MeOH-d_4) 177.1 (C-7), 168.7 (C-9′), 149.6 (C-4′), 147.1 (C-3′), 146.8 (C-7′), 127.8 (C-1′), 123.0 (C-6′), 116.5 (C-5′), 115.3 (C-2′), 115.2 (C-8′), 76.2 (C-1), 73.5 (C-5), 72.0 (C-4), 71.3 (C-3), 38.8 (C-6), 38.2 (C-2). The data correspond to chlorogenic acid.[34]

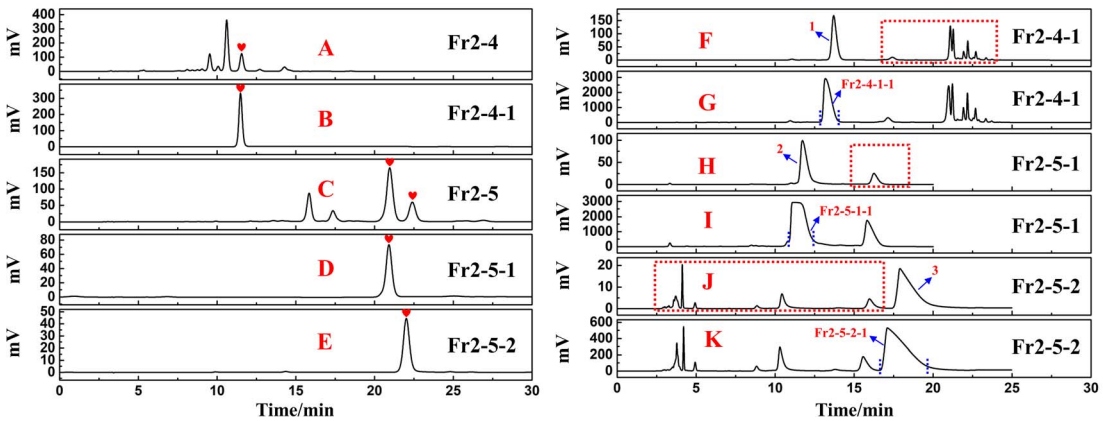

Fig. 4 HPLC reanalysis chromatogram of fractions Fr2-4 (A), Fr2-4-1 (B), Fr2-5 (C), Fr2-5-1 (D) and Fr2-5-2 (E) on ReproSil-Pur C18 AQ analytical column, optimized analytical chromatogram (F), (H) and (J) and preparative chromatogram (G), (I) and (K) of fractions Fr2-4-1, Fr2-5-1 and Fr2-5-2 on Click XIon analytical and preparative columns.

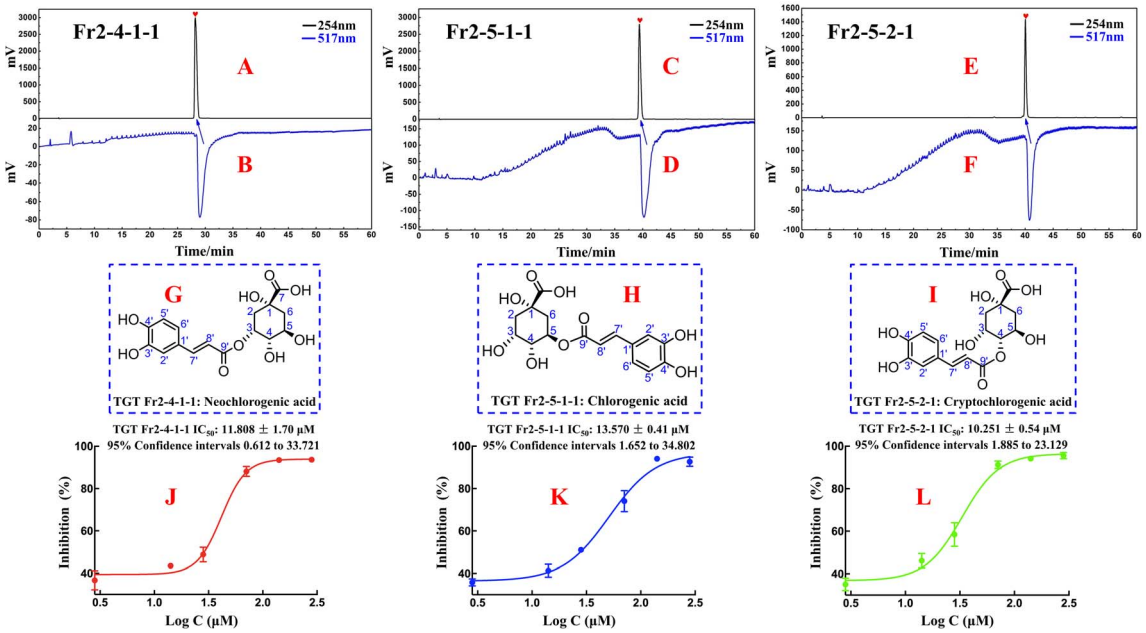

Fig. 5 Purity (A), (C) and (E), DPPH radical scavenging profile (B), (D) and (F), chemical structures (G)–(I) and DPPH inhibition activities (J)–(L) of the isolated DPPH inhibitors (Fr2-4-1-1, Fr2-5-1-1 and Fr2-5-2-1).

Fraction Fr2-5-2-1 (cryptochlorogenic acid, ESI-MS *m/z* 353.27, $[M-H]^-$, calc. for $C_{16}H_{18}O_9$ *m/z* 354.09): ^{1}H NMR (600 M*Hz*, MeOH-d_4) 7.63 (1H, d, $J = 15.9$ *Hz*, H-7′), 7.06 (1H, d, $J =$ 2.0 *Hz*, H-2′), 6.96 (1H, dd, $J = 8.2$, 2.0 *Hz*, H-6′), 6.77 (1H, d, $J =$ 8.2 *Hz*, H-5′), 6.36 (1H, d, $J = 15.9$ *Hz*, H-8′), 4.79 (1H, dd, $J = 9.3$, 3.0 *Hz*, H-3), 4.28 (1H, m, H-3, 5), 3.64 (1H, dd, $J = 8.4$, 3.2 *Hz*, H-4), 2.19 (1H, m, H-2a, 6a), 2.06 (1H, ddd, $J = 14.4$, 4.1, 2.9 *Hz*, H-2b), 2.00 (1H, dd, $J = 13.4$, 10.8 *Hz*, H-6b); ^{13}C NMR (151 M*Hz*, MeOH-d_4) 177.3 (C-7), 169.0 (C-9′), 147.1 (C-7′), 146.8 (C-3′), 127.9 (C-1′), 123.0 (C-6′), 116.5 (C-5′), 115.4 (C-8′), 115.1 (C-2′), 79.3 (C-4), 76.6 (C-1), 69.6 (C-3), 65.5 (C-5), 42.7 (C-6), 38.4 (C-2). The data correspond to cryptochlorogenic acid.[35]

3.3 Antioxidant activity of the isolated DPPH inhibitors and their structure–activity relationships

To evaluate the *in vitro* DPPH scavenging activities of the isolated DPPH inhibitors Fr2-4-1-1 (neochlorogenic acid, NCGA), Fr2-5-1-1 (chlorogenic acid, CGA) and Fr2-5-2-1 (cryptochlorogenic acid, CCGA), DPPH free radical scavenging assays were performed in this study with a modified method based on Dehghan *et al.* with some modifications. As shown in Fig. 5J–L, the three isolated DPPH inhibitors (NCGA, CGA and CCGA) displayed strong DPPH scavenging activity, with IC_{50} values of 11.808 ± 1.70 μM, 13.570 ± 0.41 μM and 10.251 ± 0.54 μM, respectively.

Compared with the structures of NCGA, CGA and CCGA, which are characterized by similarity of the parent nuclei and are distinguished by the position of the caffeoyl substituent, the caffeoyl substituted C4 quinic acid (CCGA) had a lower IC_{50} value (10.251 ± 0.54 μM) than the caffeoyl substituted C3/C5 quinic acid. As shown in Fig. 2B1–B3 and 4A–E, the peak orders of NCGA, CGA and CCGA on the ReproSil-Pur C18 AQ column were NCGA (caffeoyl substituted C3 quinic acid), CGA (caffeoyl substituted C5 quinic acid) and CCGA (caffeoyl substituted C4 quinic acid), which indicated that the polarites of the three 3-caffeoylquinic acid isomers were as follows: NCGA (caffeoyl substituted C3 quinic acid) > CGA (caffeoyl substituted C5 quinic acid) > CCGA (caffeoyl substituted C4 quinic acid). In addition, the peak orders of NCGA, CGA and CCGA on the Click XIon column (Fig. 4F–K) were CGA (caffeoyl substituted C5 quinic acid), NCGA (caffeoyl substituted C3 quinic acid) and CCGA (caffeoyl substituted C4 quinic acid), which indicated that the hydrophilia of the three 3-caffeoylquinic acid isomers decreased in the following order: CCGA (caffeoyl substituted C4 quinic acid) > NCGA (caffeoyl substituted C3 quinic acid) > CGA (caffeoyl substituted C5 quinic acid). The DPPH scavenging activity sequences of the caffeoyl substituted C3/C4/C5 quinic acid should be CCGA (caffeoyl substituted C4 quinic acid) > NCGA (caffeoyl substituted C3 quinic acid) > CGA (caffeoyl substituted C5 quinic acid). These results suggest that the difference in antioxidant activity present among NCGA, CGA and CCGA is influenced by the position of the caffeoyl substituent. This difference may be due to differences in spatial site resistance.

3.4 Effects of 3-caffeoylquinic acid isomers on cardiac function during myocardial I/R

To determine the cardioprotective effects of 3-caffeoylquinic acid isomers on MIRI, isolated mouse hearts were perfused with each compound at a concentration of 5.0 μM in K–H buffer for 15 min using the Langendorff model before ischaemia was simulated by stopping perfusion for 25 min, following 45 min of reperfusion. The function of isolated hearts in different groups was recorded, and the results are shown in Fig. 6. When the myocardium

undergoes I/R, it results in impaired cardiac function and causes hemodynamic disturbances.[36] The heart's left ventricular internal pressure and its rate of change are important indicators reflecting and evaluating the systolic and diastolic functions of the left ventricle.[37] The rate pressure product (RPP) and +dP/dt mainly reflect the systolic function of the left ventricle; the LVDP and −dP/dt mainly reflect the diastolic function of the left ventricle. Increasing duration of ischemia causes progressive irreversible injury. Morphologically, this irreversible injury is characterized by glycogen depletion, margination of nuclear chromatin, mitochondrial swelling and sarcolemmal breaks. Myocardial reperfusion accentuates these changes and induces the appearance of myofibrillar contraction band. As a result, myocardial contractile function, diastolic function, and compliance was decreased, and the ventricles became stiff and difficult to dilate.[38] In the I/R group, heart reperfusion after 25 min of ischemia caused severe myocardial injury in the hearts of mice. Specifically, compared with those in the contral group, the LVDP, RPP, +dP/dt, and −dP/dt in the treated group were strongly significantly lower ($^{###}P < 0.001$). These findings indicate that left ventricular contractility and relaxation are significantly reduced during reperfusion, which severely affects the recovery of cardiac function. Overall, pretreatment with 3-caffeoylquinic acid isomers (CGA, NCGA and CCGA) did not affect myocardial contractility or cardiac function compared with that in I/R hearts. As shown in Table 1 and Fig. 6, at the end of 45 min of reperfusion, the LVDP, RPP, +dP/dt and −dP/dt were significantly greater and significantly different in the CCGA group than in the I/R group ($^{*}P < 0.05$), suggesting that CCGA could significantly attenuate the myocardial damage caused by MIRI (CCGA group: LVDP = 59.84 ± 18.42 mm_{Hg}, RPP = 19 095.11 ± 5982.75 mm_{Hg} per beats per min, +dP/dt = 1787.63 ± 609.91 mm_{Hg} s^{-1}, −dP/dt = −1405.94 ± 562.67 mm_{Hg} s^{-1}; I/R group: LVDP = 39.59 ± 20.13 mm_{Hg}, RPP = 8941.54 ± 5053.79 mm_{Hg} per beats per min, +dP/dt = 1094.72 ± 458.97 mm_{Hg} s^{-1}, −dP/dt = −895.40 ± 401.41 mm_{Hg} s^{-1}). In addition, as the reperfusion duration increased, the changes in each index showed a decreasing trend and gradually stabilized. CCGA significantly attenuated the effects of I/R on hemodynamic cardiac function in mice. These data demonstrated, to some extent, the protective effect of CCGA on MIRI in the hearts of mice.

3.5 Effects of 3-caffeoylquinic acid isomers on I/R-induced cardiomyocyte damage in heart tissue

Heart failure is a clinical syndrome characterized by a decrease in forward cardiac output due to dysfunction in cardiac systolic or diastolic function, which is insufficient to meet systemic

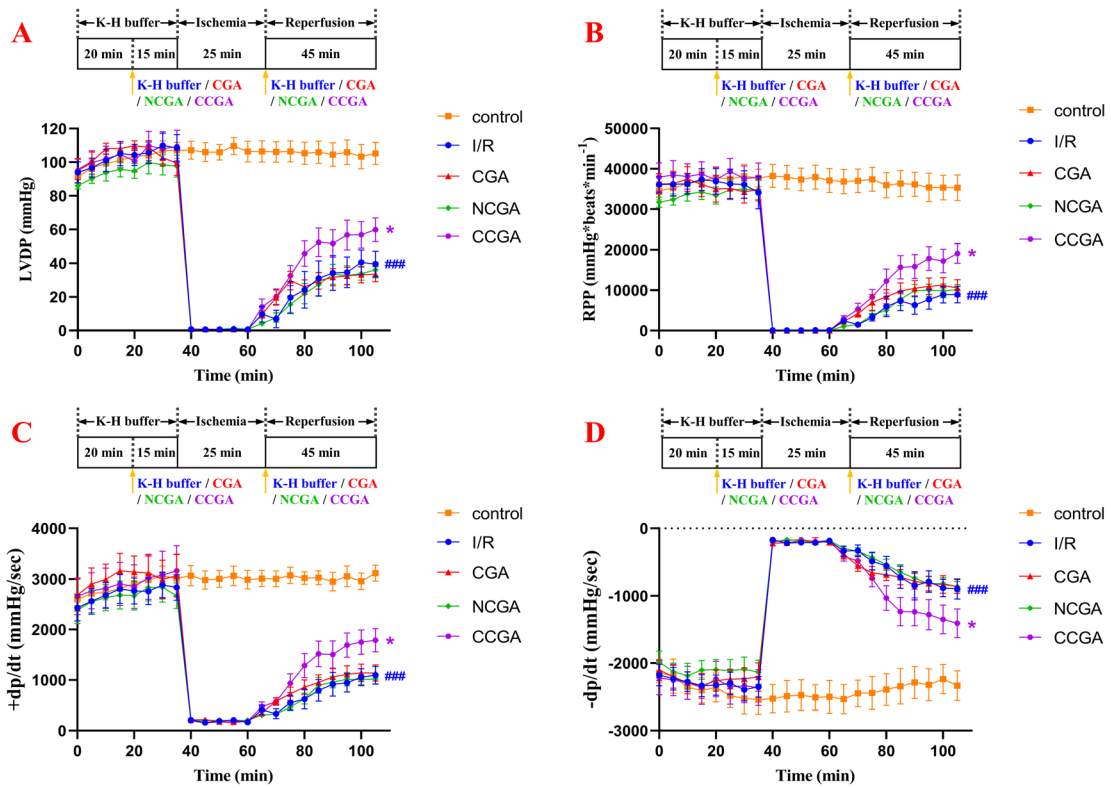

Fig. 6 (A) Left ventricular developed pressure (LVDP) in isolated normal hearts with I/R injury to the heart, CGA-treated I/R injury to the heart, NCGA-treated I/R injury to the heart, and CCGA-treated I/R injury to the heart. (B) Rate pressure product (RPP) in isolated normal hearts with I/R injured heart, CGA-treated I/R injured heart, NCGA-treated I/R injured heart and CCGA-treated I/R injured heart. (C) Maximum rate of pressure rise within the left ventricle during isovolumic systole (+dP/dt) in isolated normal hearts, I/R-injured hearts, CGA-treated I/R-injured hearts, NCGA-treated I/R-injured hearts and CCGA-treated I/R-injured hearts. (D) Maximum rate of isovolumic diastolic left ventricular pressure drop (−dP/dt) in isolated normal hearts, I/R-injured hearts, CGA-treated I/R-injured hearts, NCGA-treated I/R-injured hearts, and CCGA-treated I/R-injured hearts. Data are presented as the mean ± SEM ($n = 6$ for the control group, $n = 7$ for the I/R group). (###$p < 0.001$ *vs.* control group; *$p < 0.05$ *vs.* I/R group).

Table 1 Effect of 3-caffeoylquinic acid isomers (CGA, NCGA and CCGA) on cardiac function in mice subjected to I/R after 45 min of reperfusion. The data are expressed as the mean ± SEM ($n = 6$ for the control group, $n = 7$ for the I/R group)

	Indicators			
Groups	LVDP (mm_{Hg})	RPP (mm_{Hg} per beats per min)	+dP/dt (mm_{Hg} s^{-1})	−dP/dt (mm_{Hg} s^{-1})
Control	105.27 ± 16.33	35 312.15 ± 7723.67	3118.60 ± 381.91	−2333.73 ± 541.11
I/R	39.59 ± 20.13	8941.54 ± 5053.79	1094.72 ± 458.97	−895.40 ± 401.41
CGA	33.52 ± 11.99	10 505.11 ± 5146.87	1138.01 ± 423.58	−858.57 ± 274.12
NCGA	36.06 ± 12.33	10 165.39 ± 3061.88	1023.02 ± 272.77	−861.19 ± 198.16
CCGA	59.84 ± 18.42	19 095.11 ± 5982.75	1787.63 ± 609.91	−1405.94 ± 562.67

metabolic needs, and backward failure. The etiology includes both initial and secondary injury factors, and myocardial ischemia has become the primary factor leading to heart failure. Cardiac remodeling is a landmark change in the occurrence and development of heart failure, which is closely related to the deterioration of cardiac function. We observed that compared to the control group, the heart was significantly enlarged in the model group. Histopathological changes in heart tissue were evaluated frequently by H&E staining. As shown in Fig. 7, the H&E staining results revealed the extent of myocardial tissue damage in the mouse model. Among them, the control group exhibited a significantly ordered and compact arrangement of myocardial fibres, the nuclei were clear, and the amount of extracellular matrix observed was notably decreased, whereas cardiomyocytes in the model group (I/R group) exhibited uneven local staining, structural damage, disordered myocardial fibre arrangement, and abnormal cellular morphology, as illustrated by the decrease in purple stained areas. In addition, the protective effects of CGA, NCGA, and CCGA on myocardial tissue injury in the hearts of mice were further investigated. Under a light microscope, it was observed that CCGA treatment rescued these pathological changes and reduced the occurrence and development of cardiac remodeling, but the other two compounds were not obvious.

3.6 Effects of 3-caffeoylquinic acid isomers on mitochondrial dynamics in I/R hearts

In the present study, CCGA administration after myocardial ischemia was found to reduce the extent of myocardial injury in the hearts of mice *in vivo*. CCGA was capable of substantially improved the overall recovery of cardiac function. Maintaining the mitochondrial mass balance is essential for restoring cardiac function after injury. Some clinical and basic studies have noted that ischemic preconditioning is associated directly with preservation of ATP after I/R, corroborating the importance of mitochondria in reperfusion injury.[39,40] However, cytoprotective mechanisms underlying ischemic preconditioning are multifactorial, such as stimulates autophagic flux by AMPK and PI3-kinase activation and mTOR inhibition.[41] Preconditioning stimulates autophagic flux by AMPK and PI3-kinase activation and mTOR inhibition. Autophagy, which is present at a certain level at the basal level, is involved in the elimination of damaged structures within the cell. Activation of autophagy in cardiomyocytes has been shown to protect against I/R damage. In contrast, excessive autophagy disrupts organelles and proteins, causing dysfunction of the organs.[42] Mitochondrial biogenesis and autophagy, the removal of aged or damaged mitochondria, are two opposing biological processes that are

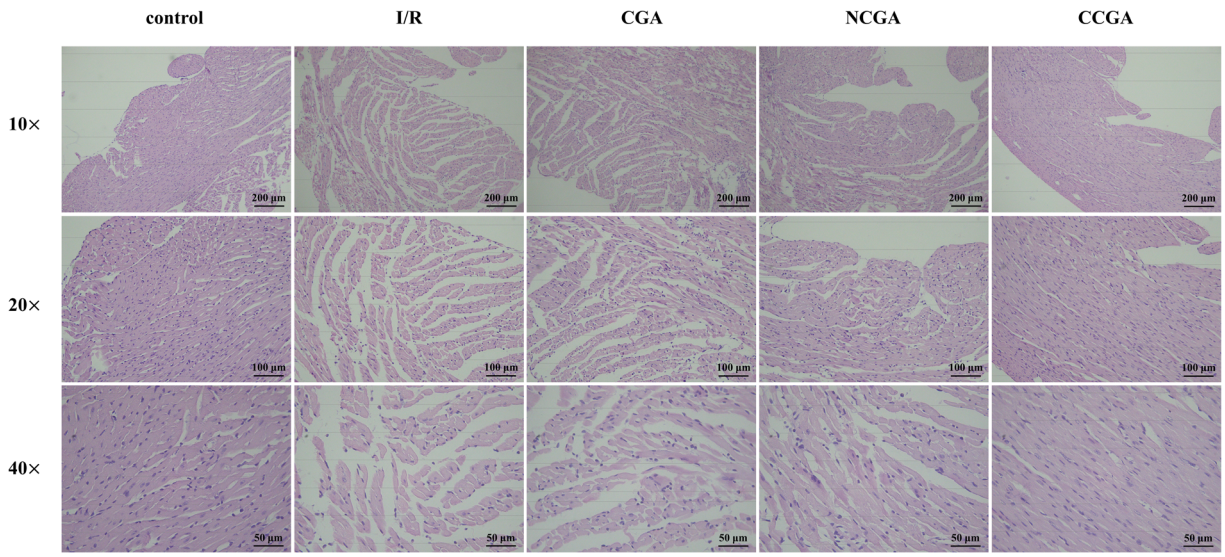

Fig. 7 H&E staining results of mouse myocardium (magnification 10× (scale bar = 200 μm), 20× (scale bar = 100 μm), and 40× (scale bar = 50 μm)).

critical for mitochondria to maintaining functional homeostasis in mitochondria.[43] When mitochondria are dysfunctional, mitochondrial biogenesis is abnormal. To further investigate the link between the protective effect of CCGA against mitochondrial functional impairment caused by I/R in the hearts of mice and mitochondrial quality control, we assessed the expression levels of mitochondria-associated proteins in response to MIRI induced by CGA, NCGA and CCGA. As shown in Fig. 8, the levels of sirt1 ($^{###}P < 0.001$), PGC-1α ($^{##}P < 0.01$), Nrf1 ($^{###}P < 0.001$), and TFAM ($^{###}P < 0.001$) in the IR group were significantly lower than those in the control group, and the expression levels of Mfn2 ($^{###}P < 0.001$) and Drp1 ($^{###}P < 0.001$) were also significantly lower, indicating that I/R led to disrupted mitochondrial homeostasis and an imbalance in mitochondrial fusion and division, resulting in myocardial injury. PGC-1α plays a key role in mitochondrial biogenesis. PGC-1α recruits transcription factors, thereby promoting mitochondrial transcription and expression. In addition, PGC-1α binds to Nrf1, which induces mitochondrial biogenesis and regulates energy metabolism. Nrf1 in turn activates transcription factor A (TFAM), which regulates mtDNA transcription and replication. Activation of transcription factors of mitochondrial genes and upregulation of local translation of proteins are associated with mitochondrial biogenesis.[44] PGC-1α can also be regulated by an upstream molecule, sirt1.[33] Sirt1 is a recognized member of the third subfamily of the histone deacetylase family and can deacetylate and thus activate PGC-1α in an NAD^+-dependent manner. The expression levels of sirt1 ($^{**}P < 0.01$), PGC-1α ($^{**}P < 0.01$), Nrf1 ($^{**}P < 0.01$), and TFAM ($^{***}P < 0.001$) were significantly elevated by treatment with CCGA. Mitochondria are highly dynamic organelles, and the dynamic balance between fission and fusion is one of the important links for mitochondria to perform their normal physiological functions.[45] Drp1 is a key protein factor regulating mitochondrial division. Mfn2 is a key molecule that regulates the fusion of the outer mitochondrial membrane. Mitochondria change their shape, number and size through constant fusion and fission to meet the demands of cellular metabolism.[46] The expression levels of Mfn2 ($^{**}P < 0.01$) and Drp1 ($^{*}P < 0.05$) in injured mouse myocardial tissues treated with CCGA were significantly elevated and even comparable to the protein expression levels in the control group. Closer inspection revealed that the degree to which Drp1 protein expression was restored in CCGA-treated cardiomyocytes was slightly weaker than the degree to which Mfn2 protein expression was restored. In contrast, the expression levels of each protein (sirt1, PGC-1α, Nrf1, TFAM, Mfn2, and Drp1) in the myocardial tissues of CGA-treated and NCGA-treated mice were not significantly different from those in the I/R group. Caffeoyl-substituted C5 quinic acid (CGA) and caffeoyl-substituted C3 quinic acid (NCGA) were less effective than caffeoyl-substituted C4 quinic acid (CCGA) in the recovery of MIRI. The position of the caffeoyl substituent affects not only the antioxidant activity of the 3-caffeoylquinic acid isomer but also the degree of recovery from myocardial injury. These results demonstrated the structural advantages of caffeoyl-substituted C4 quinic acid. Furthermore, the sirt1/PGC-1α/Nrf1/TFAM signalling pathway is likely to play a critical role in mediating the interaction between CCGA processing and mitochondrial dynamics.

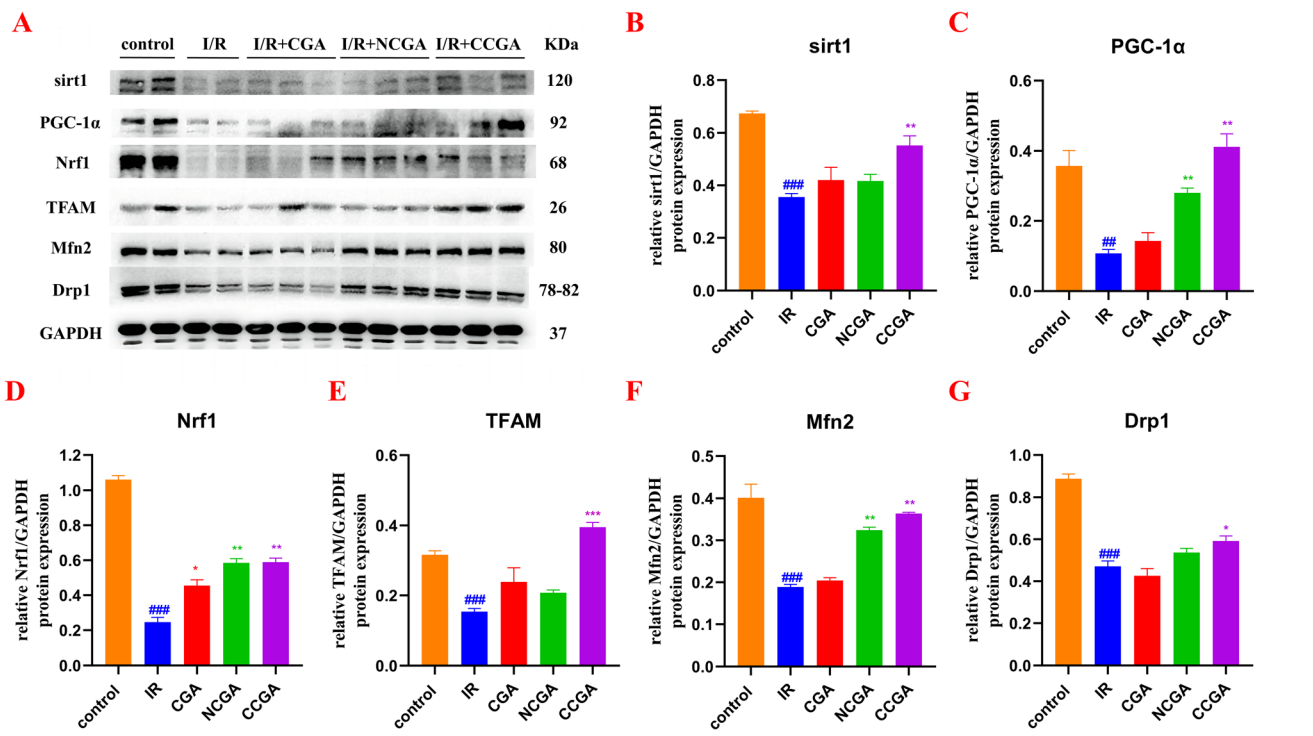

Fig. 8 Expression of sirt1, PGC-1α, Nrf1, TFAM, Mfn2, and Drp1 in ischemic myocardial tissue. (#$p < 0.05$, ##$p < 0.01$, ###$p < 0.001$ *vs.* control group; *$p < 0.05$, **$p < 0.01$, ***$p < 0.001$ *vs.* I/R group).

4 Study limitations

In this study, we studied the effects of myocardial mitochondrial biogenesis on myocardial cells by studying the Langendorff modle model of acute ischemial-reperfusion injury in isolated hearts. The effect of CCGA (caffeoyl-substituted C4 quinic acid) on MIRI was revealed through sirt1/PGC-1α/Nrf1/TFAM signaling pathway. Although these studies on the protective effect of CCGA in cardiac I/R are relatively preliminary, the evidence for its beneficial effects is encouraging. However, due to the limitation of our current experimental equipment, we cannot use whole animals to conduct relevant studies on Na^+/K^+-ATPase activity, liver and other tissue metabolism, and myocardial cell post-infarction regional remodeling strain caused by left ventricular dysfunction after myocardial ischemia-reperfusion. In addition, the safety of CCGA in treating MIRI remains to be determined. Therefore, we will further confirm the effect of CCGA on MIRI through more designs and studies in the future.

5 Conclusions

In the present study, the DPPH inhibitors of 3-caffeoylquinic acid isomers isolated from *S. tangutica* exhibited different degrees of antioxidant activity and MIRI protection. MPLC, the online HPLC–DPPH technique and two-dimensional liquid chromatography were used for enrichment, screening and preparation to finally obtain neochlorogenic acid (NCGA, 18.5 mg), chlorogenic acid (CGA, 81.7 mg) and cryptochlorogenic acid (CCGA, 15.0 mg), respectively. The free radical scavenging activity and purity of these three 3-caffeoylquinic acid isomers were also evaluated. NCGA, CGA and CCGA all exhibited good DPPH radical scavenging activity, with CCGA (caffeoyl substituted C4 quinic acid) being the most effective. The purities were all greater than 95%. The results of the present study showed that the treatment of DPPH inhibitors using the described screening, isolation and purification methods is instructive for the isolation of DPPH inhibitors of the 3-caffeoylquinic acid isomer from different natural products.

This study also investigated the protective effects of 3-caffeoylquinic acid isomers against MIRI in mouse hearts for the first time. The results based on Langendorff's *in vitro* modelling showed that CCGA had good activity against MIRI changes, whereas NCGA and CGA had little protection against MIRI. Overall, there were differences in antioxidant activity and MIRI protection among the 3-caffeoylquinic acid isomers, suggesting an influence of the position of the caffeoyl substituent. Mitochondria are important organelles in heart cells, and mitochondrial dysfunction has been proven to play a major role in MIRI. The reduced expression of the mitochondrial fusion protein Mfn2 and the mitochondrial fission protein Drp1 in the MIRI model further demonstrated severe damage to myocardial mitochondrial dynamics. CCGA protection was achieved through the activation of mitochondrial biogenesis during MIRI in this study. In summary, the major findings and results of this study reveal that the CCGA has potential therapeutic value for protecting the myocardium from ischemic diseases. The mechanism of action, therapeutic window and potential side effects of this herb will be further elucidated in future studies.

Abbreviations

IHD	Ischemic heart disease
S. tangutica	*Saxifraga tangutica*
MIRI	Myocardial ischemia/reperfusion injury
DPPH	1,1-Diphenyl-2-picrylhydrazyl
NCGA	Neochlorogenic acid
CGA	Chlorogenic acid
CCGA	Cryptochlorogenic acid
I/R	Ischemia/reperfusion
TTMs	Traditional Tibetan medicines
RPLC	Reversed-phase liquid chromatography
HILIC	Hydrophilic liquid chromatography
EtOH	Ethanol
MeOH	Methanol
ACN	Acetonitrile
FA	Formic acid
OA	Oleic acid
SPF	Specific pathogen free
MPLC	Medium-pressure liquid chromatography
LV	Left ventricular
LVEDP	Left ventricular end-diastolic pressure
LVDP	Left ventricular developed pressure
PFA	Paraformaldehyde
PMSF	Phenylmethanesulfonyl fluoride
SDS–PAGE	Sodium dodecyl sulfate–polyacrylamide gel electrophoresis
SEM	Standard error of mean
ANOVA	Analysis of variance
HR-ESI-MS	High-resolution electrospray ionization-mass spectrometry
^{1}H NMR	^{1}H-Nuclear magnetic resonance
^{13}C NMR	^{13}C-Nuclear magnetic resonance
RPP rate	Pressure product

Ethical statement

All animal experiments were obtained from Jinan Pengyue Experimental Animal Breeding Co. Ltd (Jinan, China). The experimental procedures were approved by the Laboratory Animal Welfare Ethics Review Committee of Yantai University (No. YDLL2023M126) and performed strictly according to the 2011 8th edition of the Guidelines for the Care and Use of Laboratory Animals (US National Institutes of Health).

Author contributions

Yingying Tong: writing—original draft, methodology, data curation, visualization. Xiaobing Shi: writing—original draft, methodology, investigation. Lin Wang: methodology, data curation, visualization. Jia Zhou: methodology, investigation. Ming Chu: methodology, data curation. Zhenhua Wang: visualization, data curation. Jun Dang: visualization, data curation, conceptualization, formal analysis, validation, writing—review and editing, project administration, funding acquisition. Gang

Li: conceptualization, formal analysis, writing—review and editing, project administration, funding acquisition. Li, A. M. Abd El-Aty: validation, writing—review and editing.

Conflicts of interest

The authors declare that they have no known competing financial interests or personal relationships that could have appeared to influence the work reported in this paper.

Acknowledgements

This work was supported by the Young Scholars in Western China, Chinese Academy of Sciences (2022) and the Innovation Platform for the Development and Construction of Special Project of Qinghai Province (2021-ZJ-T05).

References

1 G. A. Roth, G. A. Mensah, C. O. Johnson, G. Addolorato, E. Ammirati, L. M. Baddour, N. C. Barengo, A. Z. Beaton, E. J. Benjamin, C. P. Benziger, *et al.* Global Burden of Cardiovascular Diseases and Risk Factors, 1990–2019, *J. Am. Coll. Cardiol.*, 2020, **76**(25), 2982–3021.

2 D. Sueta and K. Tsujita, JS3-6 - therapeutic strategies for ischemic heart disease, *Ann. Oncol.*, 2019, **30**(6), 9.

3 M. Y. Wu, G. T. Yiang, W. T. Liao, A. P. Y. Tsai, Y. L. Cheng, P. W. Cheng, C. Y. Li and C. J. Li, Current Mechanistic Concepts in Ischemia and Reperfusion Injury, *Cell. Physiol. Biochem.*, 2018, **46**(4), 1650–1667.

4 T. Kalogeris, C. P. Baines, M. Krenz and R. J. Korthuis, Ischemia/Reperfusion, *Comprehensive Physiology*, 2017, **7**(1), 113–170.

5 S. Cadenas, ROS and redox signaling in myocardial ischemia-reperfusion injury and cardioprotection, *Free Radicals Biol. Med.*, 2018, **117**, 76–89.

6 S. B. Ong, S. Hernández-Reséndiz, G. E. Crespo-Avilan, R. T. Mukhametshina, X. Y. Kwek, H. A. Cabrera-Fuentes and D. J. Hausenloy, Inflammation following acute myocardial infarction: multiple players, dynamic roles, and novel therapeutic opportunities, *Pharmacol. Ther.*, 2018, **186**, 73–87.

7 W. Y. Li, W. Li, Y. Leng, Y. H. Xiong and Z. Y. Xia, Ferroptosis Is Involved in Diabetes Myocardial Ischemia/Reperfusion Injury through Endoplasmic Reticulum Stress, *DNA Cell Biol.*, 2020, **39**(2), 210–225.

8 H. Zhou, P. J. Zhu, J. Wang, H. Zhu, J. Ren and Y. D. Chen, Pathogenesis of cardiac ischemia reperfusion injury is associated with CK2α-disturbed mitochondrial homeostasis via suppression of FUNDC1-related mitophagy, *Cell Death Differ.*, 2018, **25**(6), 1080–1093.

9 E. J. Lesnefsky, Q. Chen, B. Tandler and C. L. Hoppel, Mitochondrial Dysfunction and Myocardial Ischemia-Reperfusion: Implications for Novel Therapies, *Annu. Rev. Pharmacol. Toxicol.*, 2017, **57**, 535–565.

10 J. Wang and H. Zhou, Mitochondrial quality control mechanisms as molecular targets in cardiac ischemia-reperfusion injury, *Acta Pharm. Sin. B*, 2020, **10**(10), 1866–1879.

11 W. Zhang, R. C. Chen, K. Y. Xu, H. B. Guo, C. Y. Li and X. B. Sun, Protective effect of Xinmai'an tablets via mediation of the AMPK/SIRT1/PGC-1α signaling pathway on myocardial ischemia-reperfusion injury in rats, *Phytomedicine*, 2023, **120**, 155034.

12 Y. Y. Liu, T. Z. Tan, G. J. Cao, L. Shi, Y. J. Song, W. J. Shan, M. Zhang, P. P. Li, H. T. Zhou, B. Zhang, *et al.* Bergenin alleviates myocardial ischemia-reperfusion injury via SIRT1 signaling, *Biomed. Pharmacother.*, 2023, **158**, 114100.

13 M. S. Zheng, Y. L. Bai, X. Y. Sun, R. Fu, L. Y. Liu, M. S. Liu, Z. Y. Li and X. L. Huang, Resveratrol Reestablishes Mitochondrial Quality Control in Myocardial Ischemia/Reperfusion Injury through Sirt1/Sirt3-Mfn2-Parkin-PGC-1α Pathway, *Molecules*, 2022, **27**(17), 5545.

14 Y. Fei, G. Y. Zhong, X. Liu, G. Wang, Z. W. Zhang and J. F. Zhao, Microscopic identification of Tibetan medicinal herb "Songdi" (Saxifraga umbellulata var pectinata), *China J. Chin. Mater. Med.*, 2013, **38**(6), 902–908.

15 Northwest Institute of Plateau Biology, Chinese Academy of Sciences, *Annals of Tibetan Medicine*, Qinghai People's Publishing House, Xining, 1991.

16 T. Nagata, N. Win, L. L. Xiao, T. Miwa, T. Okumura, H. Fushimi, H. Morita and Y. Shimada, Anti-cancer Effect of Saxifaga stolonifera Meerb, *Clin. Exp. Pharmacol.*, 2016, **6**(3), 211.

17 J. Dang, Y. D. Tao, Y. Shao, L. J. Mei, L. Zhang and Q. L. Wang, Antioxidative extracts and phenols isolated from Qinghai-Tibet Plateau medicinal plant *Saxifraga tangutica* Engl., *Ind. Crops Prod.*, 2015, **78**, 13–18.

18 Y. L. Chang, K. Huang, F. Yang, Y. Y. Gao, Y. Zhang, S. Li, B. Liu and S. Z. Guo, Metabolites of chlorogenic acid and its isomers: metabolic pathways and activities for ameliorating myocardial hypertrophy, *J. Funct. Foods*, 2022, **96**, 105216.

19 B. Tang, Y. M. Huang, X. L. Ma, X. X. Liao, Q. Wang, X. N. Xiong and H. Li, Multispectroscopic and docking studies on the binding of chlorogenic acid isomers to human serum albumin: effects of esteryl position on affinity, *Food Chem.*, 2016, **212**, 434–442.

20 Z. R. Xu, Q. J. Cao, A. Manyande, S. B. Xiong and H. Y. Du, Analysis of the binding selectivity and inhibiting mechanism of chlorogenic acid isomers and their interaction with grass carp endogenous lipase using multi-spectroscopic, inhibition kinetics and modeling methods, *Food Chem.*, 2022, **382**, 132106.

21 Y. Zhou, The Protective Effects of Cryptochlorogenic Acid on β-Cells Function in Diabetes in vivo and vitro via Inhibition of Ferroptosis, *Diabetes, Metab. Syndr. Obes.: Targets Ther.*, 2020, **13**, 1921–1931.

22 J. Kim, S. Lee, J. Shim, H. W. Kim, J. Kim, Y. J. Jiang, H. Yang, J. Park, S. H. Choi, J. H. Yoon, K. W. Lee and H. J. Lee, Caffeinated coffee, decaffeinated coffee, and the phenolic phytochemical chlorogenic acid up-regulate NQO1 expression and prevent H_2O_2-induced apoptosis in primary cortical neurons, *Neurochem. Int.*, 2012, **60**(5), 466–474.

23 N. J. Liang and D. D. Kitts, Amelioration of Oxidative Stress in Caco-2 Cells Treated with Pro-inflammatory Proteins by Chlorogenic Acid Isomers via Activation of the Nrf2-Keap1-ARE-Signaling Pathway, *J. Agric. Food Chem.*, 2018, **66**(42), 11008–11017.

24 K. Iwai, N. Kishimoto, Y. Kakino, K. Mochida and T. Fujita, *In vitro* antioxidative effects and tyrosinase inhibitory activities of seven hydroxycinnamoyl derivatives in green coffee beans, *J. Agric. Food Chem.*, 2004, **52**(15), 4893–4898.

25 L. Aljerf and N. AlMasri, High resolution chromatography and sensitive retention: optimization of the experimental conditions for proteins extraction by preparative HPLC, *Journal of Progressive Research in Modern Physics and Chemistry*, 2018, **3**(1), 97–103.

26 Q. W. Zhang, L. G. Lin and W. C. Ye, Techniques for extraction and isolation of natural products: a comprehensive review, *Chin. Med.*, 2018, **13**, 20.

27 J. L. Cao, S. S. Wang, H. Hu, C. W. He, J. B. Wan, H. X. Su and Y. T. Wang, Online comprehensive two-dimensional hydrophilic interaction chromatography × reversed-phase liquid chromatography coupled with hybrid linear ion trap Orbitrap mass spectrometry for the analysis of phenolic acids in *Salvia miltiorrhiza*, *J. Chromatogr. A*, 2018, **1536**, 216–227.

28 Y. Z. Dawa, Y. R. Du, Q. Wang, C. B. Chen, D. L. Zou, D. S. Qi, J. B. Ma and J. Dang, Targeted isolation of 1,1-diphenyl-2-picrylhydrazyl inhibitors from *Saxifraga atrata* using medium- and high-pressure liquid chromatography combined with online high performance liquid chromatography-1,1-diphenyl-2-picrylhydrazyl detection, *J. Chromatogr. A*, 2021, **1635**, 461690.

29 H. Dehghan, P. Salehi and M. S. Amiri, Bioassay-guided purification of α-amylase, α-glucosidase inhibitors and DPPH radical scavengers from roots of *Rheum turkestanicum*, *Ind. Crops Prod.*, 2018, **117**, 303–309.

30 H. Ma, J. Y. Wang, D. P. Thomas, C. Tong, L. Leng, W. K. Wang, M. Merk, S. Zierow, *et al.* Impaired Macrophage Migration Inhibitory Factor-AMP-Activated Protein Kinase Activation and Ischemic Recovery in the Senescent Heart, *Circulation*, 2010, **122**(3), 282–292.

31 A. T. Melese, D. T. Ayele, L. Aljerf, D. F. Al-Fekaiki and M. L. Akele, Investigating the phytoavailability of metals in roots of *Croton macrostachyus* and *Phytolacca dodecandra*: induced rhizosphere processes, *BioMetals*, 2023, **36**, 1347–1359.

32 P. N. Chuah, D. Nyanasegaram, K. X. Yu, R. R. Mohamed, S. Al-Dhalli, C. S. Kue, K. Shaari and C. H. Ng, Comparative conventional extraction methods of ethanolic extracts of *Clinacanthus nutans* leaves on antioxidant activity and toxicity, *Br. Food J.*, 2020, **122**(10), 3139–3149.

33 S. S. Sun, X. L. Xin, L. J. Zhu, L. Chen, Z. C. Xu and Y. F. Liu, Preparative separation of five polyphenols from the fruits of *Sorbus pohuashanensis* Hedl. by high-speed counter-current chromatography, *J. Chromatogr. B*, 2021, **1172**, 122620.

34 B. Ahmad, M. Rizwan, A. Rauf, M. Raza, S. Bashir, J. Molnár, A. Csonka, D. Szabó, M. S. Mubarak, *et al.* Isolation of Chlorogenic Acid from Soil Borne Fungi Screlotium rolfsii, Their Reversal of Multidrug Resistance and Anti-proliferative in Mouse Lymphoma Cells, *Med. Chem.*, 2017, **13**(8), 721–726.

35 W. M. Hu and D. P. Xu, Identification of anti-hyperuricemic components from *Cichorium intybus* L. taproots, *Food Biosci.*, 2023, **56**, 103145.

36 L. De Roeck, S. Vandamme, B. R. Everaert, V. Hoymans, S. Haine, T. Vandendriessche, J. Bosmans, M. W. Ronsyn, H. Miljoen, A. Van Berendoncks, *et al.* Adiponectin and ischemia-reperfusion injury in ST segment elevation myocardial infarction, *Eur. Heart J.*, 2016, **5**(1), 71–76.

37 X. Q. Sun, S. Chen, L. F. Wang and Z. W. Chen, Total flavones of *Rhododendron simsii* Planch flower protect isolated rat heart from ischaemia-reperfusion injury and its mechanism of UTR-RhoA-ROCK pathway inhibition, *J. Pharm. Pharmacol.*, 2018, **70**(12), 1713–1722.

38 G. Heusch, Myocardial ischaemia-reperfusion injury and cardioprotection in perspective, *Nat. Rev. Cardiol.*, 2020, **17**(12), 773–789.

39 R. Behera, V. Sharma, A. K. Grewal, A. Kumar, B. Arora, A. Najda, G. M. Albadrani, A. E. Altyar, M. M. Abdel-Daim and T. G. Singh, Mechanistic correlation between mitochondrial permeability transition pores and mitochondrial ATP dependent potassium channels in ischemia reperfusion, *Biomed. Pharmacother.*, 2023, **162**, 114599.

40 H. H. Szeto, S. Y. Liu, Y. Soong, D. L. Wu, S. F. Darrah, F. Y. Cheng, Z. H. Zhao, M. Ganger, C. Y. Tow and S. V. Seshan, Mitochondria-Targeted Peptide Accelerates ATP Recovery and Reduces Ischemic Kidney Injury, *J. Am. Soc. Nephrol.*, 2011, **22**(6), 1041–1052.

41 K. L. Go, S. Lee, L. Zendejas, K. E. Behrns and J. S. Kim, Mitochondrial Dysfunction and Autophagy in Hepatic Ischemia/Reperfusion Injury, *BioMed Res. Int.*, 2015, **2015**, 183469.

42 M. Gunata and H. Parlakpinar, A review of myocardial ischaemia/reperfusion injury: pathophysiology, experimental models, biomarkers, genetics and pharmacological treatment, *Cell Biochem. Funct.*, 2021, **39**(2), 190–217.

43 L. D. Popov, Mitochondrial biogenesis: an update, *J. Cell. Mol. Med.*, 2020, **24**(9), 4892–4899.

44 S. Nemoto, M. M. Fergusson and T. Finkel, SIRT1 functionally interacts with the metabolic regulator and transcriptional coactivator PGC-1α, *J. Biol. Chem.*, 2005, **280**(16), 16456–16460.

45 E. L. Mills, B. Kelly and L. A. J. O'Neill, Mitochondria are the powerhouses of immunity, *Nat. Immunol.*, 2017, **18**(5), 488–498.

46 M. J. Calkins, M. Manczak, P. Z. Mao, U. Shirendeb and P. H. Reddy, Impaired mitochondrial biogenesis, defective axonal transport of mitochondria, abnormal mitochondrial dynamics and synaptic degeneration in a mouse model of Alzheimer's disease, *Hum. Mol. Genet.*, 2011, **20**(23), 4515–4529.